iScience

CellPress
OPEN ACCESS

Article

MNSs-mediated N-glycan processing is essential for auxin homeostasis in *Arabidopsis* roots during alkaline response

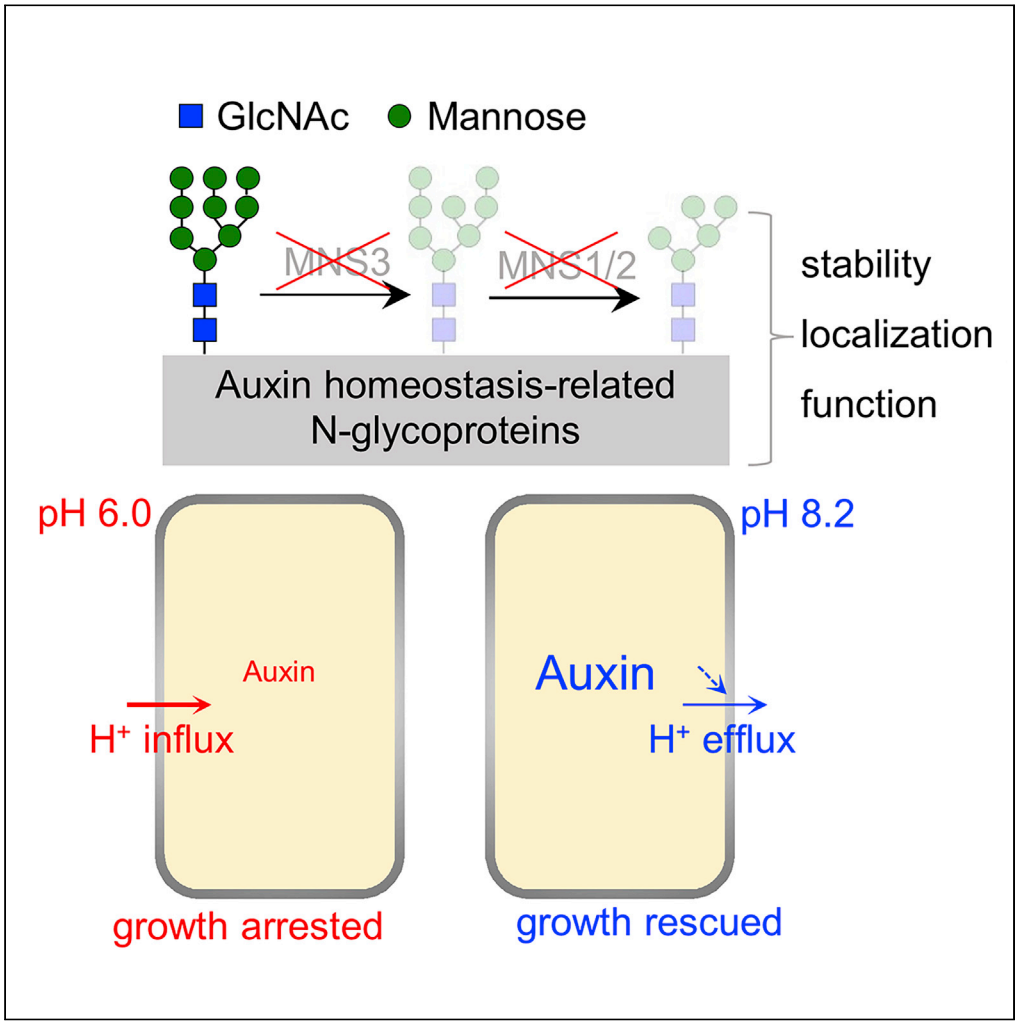

Tianyu Xia, Yujie Zhan, Yangjie Mu, Jianhua Zhang, Weifeng Xu

wfxu@fafu.edu.cn

Highlights

Root growth inhibition of the *mns1 mns2 mns3* mutant was rescued at alkaline pH

Auxin homeostasis was changed between normal and alkaline pH in *mns1 mns2 mns3*

Disrupting auxin transport inhibited the alkaline-rescued root growth in *mns1 mns2 mns3*

Xia et al., iScience 25, 104298
May 20, 2022
https://doi.org/10.1016/j.isci.2022.104298

iScience

CellPress
OPEN ACCESS

Article

MNSs-mediated N-glycan processing is essential for auxin homeostasis in *Arabidopsis* roots during alkaline response

Tianyu Xia,[1] Yujie Zhan,[1] Yangjie Mu,[1] Jianhua Zhang,[2] and Weifeng Xu[1,3,*]

SUMMARY

Early steps in the endoplasmic reticulum (ER) lumen and *cis*-Golgi comprise trimming of N-glycans by class I α-mannosidases (MNSs) play crucial roles in root growth and stress response. Herein, we found that the root growth inhibition in the *mns1 mns2 mns3* mutant was partially rescued under alkaline condition, and inhibitor treatment to disrupt auxin transport counteracted this alkaline-maintained root growth. Further study showed that indole-3-acetic acid (IAA) levels were undetectable in *mns1 mns2 mns3* at normal condition and recovered at alkaline condition, which corroborate our N-glycopeptide profiling, from which N-glycopeptides related with IAA biosynthesis, amino acid conjugates hydrolysis, and response showed differential abundance between normal and alkaline conditions in *mns1 mns2 mns3*. Overall, our results linked the need for MNSs-mediated N-glycan processing in the ER and *cis*-Golgi with maintenance of auxin homeostasis and transport in *Arabidopsis* roots during the response to alkaline stress.

INTRODUCTION

Asparagine (N)-linked glycosylation is a major co- and post-translational protein modification in eukaryotes and plays crucial roles in protein folding, quality control, and sorting (Helenius and Aebi, 2001). The biosynthesis of protein-linked glycans starts in ER by transfer of the $Glc_3Man_9GlcNAc_2$ (where Glc is glucose, Man is mannose, and GlcNAc is N-acetylglucosamine) oligosaccharide from the lipid-linked precursor to N residue within the sequence motif NxS/T (x represents any amino acid except proline, and S/T represents serine and threonine) of nascent polypeptide (Kornfeld and Kornfeld, 1985). Subsequent N-glycan processing involves a series of highly coordinated step-by-step enzymatic conversions occurring in the ER and Golgi. The first N-glycan processing step is the removal of three glucosyl residues from $Glc_3Man_9GlcNAc_2$ to generate $Man_9GlcNAc_2$, and then four α-1,2-mannose residues are trimmed to generate the $Man_5GlcNAc_2$, which is further processed for the formation of complex N-glycans (Strasser, 2014). In *Arabidopsis*, the α-1,2-mannose trimming is carried out by one ER class I α-mannosidase (MNS3) and two *cis*-Golgi class I α-mannosidases (MNS1 and MNS2) (Liebminger et al., 2009). Several evidences showed that MNSs-mediated N-glycan processing plays important roles in root development, cell wall biosynthesis, and salt tolerance (Liebminger et al., 2009; Liu et al., 2018; Veit et al., 2018). For example, mutants defective in *MNS1* and *MNS2* showed more salt-sensitive root phenotypes than the wild type (WT), whereas the *mns1 mns2 mns3* triple mutants accumulated $Man_9GlcNAc_2$ structures and displayed short, radially swollen roots and abnormal cell walls (Liebminger et al., 2009; Nagashima et al., 2018).

Soil alkalinity is one of the most severe environmental problems and limits crop yield significantly. Under alkaline stress, high pH is the major factor that limits root growth and development during the life cycle of the plant (Guo et al., 2010). Several reported evidences have shown that the plasma membrane (PM) H^+-ATPase-mediated proton extrusion plays a crucial role in the adaptation of *Arabidopsis* roots to alkaline stress. SOS2-LIKE PROTEIN KINASE5 (PKS5, also known as CIPK11 or SnRK3.22) can phosphorylate Ser-931 to inhibit PM H^+-ATPase activity by preventing interaction with 14-3-3 protein, and loss of *PKS5/CIPK11/SnRK3.22* function increases plant tolerance to alkaline stress (Fuglsang et al., 2007). In the absence of chaperone J3, which interacts with and represses *PKS5/CIPK11/SnRK3.22* kinase activity, plant tolerance to alkaline pH decreases (Yang et al., 2010). Auxin activates the PM H^+-ATPase via increasing the phosphorylation of its penultimate threonine or repressing the activities of protein phosphatase type C proteins (Spartz et al., 2014; Takahashi et al., 2012). These results showed that protein phosphorylation is involved

[1]Center for Plant Water-use and Nutrition Regulation and College of Life Sciences, Joint International Research Laboratory of Water and Nutrient in Crop and College of Resource and Environment, Fujian Agriculture and Forestry University, Jinshan, Fuzhou 350002, China

[2]Department of Biology, Hong Kong Baptist University, Kowloon Tong, Hong Kong, China

[3]Lead contact

*Correspondence: wfxu@fafu.edu.cn

https://doi.org/10.1016/j.isci.2022.104298

in the adaptation of *Arabidopsis* roots to alkaline stress via regulating PM H^+-ATPase. In addition, Ladwig et al. (2015) revealed that PM H^+-ATPases (AHA1 and AHA2) form a functional cation-translocating unit with CYCLIC NUCLEOTIDE-GATED CHANNEL17 (CNGC17) to participate in cell expansion through proton extrusion and cation influx (Ladwig et al., 2015). This unit was activated by the receptor-like kinases PHYTOSULFOKINE RECEPTOR1 (PSKR1) and BRI-ASSOCIATED RECEPTOR KINASE1 (BAK1) (Ladwig et al., 2015), whose biogenesis and/or function are prone to perturbations by compromised ER N-glycosylation (Nagashima et al., 2018), suggesting a link between the PM H^+-ATPase and N-glycosylated receptor-like kinases. However, the potential roles of N-glycosylation in alkaline response are still unclear.

In this study, we uncovered the function of N-glycan processing in plant response to alkaline stress by using the class I α-mannosidases-deficient *Arabidopsis* lines. We found that the root growth inhibition of the *mns1 mns2 mns3* mutant was partially rescued when grown on media at high pH. Pharmacological experiment, noninvasive ion flux measurement, and N-glycoproteomic analyses were performed to elucidate the phenomenon of the alkaline-maintained root growth in *mns1 mns2 mns3*. Finally, we linked the need for α-mannosidase-mediated N-glycan processing in the ER and Golgi with maintenance of auxin homeostasis and transport in *Arabidopsis* roots during the response to alkaline stress.

RESULTS

Root growth of the *mns1 mns2 mns3* mutant was maintained under alkaline pH

To investigate the potential roles of protein N-glycosylation in acidic or alkaline stress, we examined the effects of external pH alteration on *mns3*, the *mns1 mns2* double mutant, and *mns1 mns2 mns3* triple mutant plants, which are defective in α-1,2-mannosidases that function in mannose trimming of N-glycans in ER (MNS3) and/or *cis*-Golgi (MNS1 and MNS2). WT, *mns3*, *mns1 mns2*, and *mns1 mns2 mns3* seeds were germinated and grown on 1/2 Murashige and Skoog (MS) medium at pH 4.5, 6.0, 7.5, or 8.2 for 10 days. The root growth of WT was significantly inhibited under acidic (pH 4.5) and alkaline (pH 8.2) stresses compared to the normal condition (pH 6.0), and similar acidic and alkaline stress responses were observed in *mns3* and the *mns1 mns2* double mutant (Figures 1A and 1C). By contrast, the *mns1 mns2 mns3* triple mutant plants displayed severe root phenotypes under standard pH 6.0 (Figure 1A), which is consistent with the previous finding (Liebminger et al., 2009). Surprisingly, the root growth and root tip structures of the *mns1 mns2 mns3* mutant were partially rescued at alkaline pH (Figures 1A, 1C and S1A), indicating that external pH is able to influence the root phenotypes of the *mns1 mns2 mns3* mutant.

Next, we analyzed the root phenotypes of the WT on ½ MS medium supplemented with kifunensine (Kif), a widely used inhibitor of α-1,2-mannosidases (Tokunaga et al., 2000), which mimics the deficiencies of the *mns1 mns2 mns3* triple mutant. The Kif-treated WT seedlings exhibited an aberrant root growth phenotype with shortened and swollen root at normal pH 6.0 and a greatly rescued root morphology at alkaline pH 8.2, whereas the Kif-treated *mns1 mns2 mns3* seedlings showed no significant changes compared to the mock control at pH 6.0 and pH 8.2 (Figures 1B, 1D; S1B). These results indicated that the alkaline-maintained root phenotypes of the *mns1 mns2 mns3* triple mutant were indeed caused by the lack of α-1,2-mannosidases.

Proton efflux in the *mns1 mns2 mns3* root tip recovered under alkaline condition

It has been shown that proton fluxes in plant roots play critical roles in maintaining root growth and facilitating plant responses to multiple stresses, including alkaline stress (Siao et al., 2020). To investigate whether alkaline pH may restore root growth in the *mns1 mns2 mns3* mutant, we measured the net proton fluxes using noninvasive ion flux measurements. We found that no significant difference in the proton efflux was detected at the elongation zone of the 10-day-old WT primary root tips between the normal and alkaline pH; by contrast, a proton influx was observed at the primary root tip elongation zone of the *mns1 mns2 mns3* mutant at normal pH 6.0, and a proton efflux was detected at alkaline pH 8.2 (Figure 2A), indicating a conversion of proton flux from inward to outward induced by alkaline treatment. These results corroborated the notion that proton secretion in root tips may play a crucial role in the alkaline-maintained root growth in *mns1 mns2 mns3*. Proton efflux in the root tip is primarily driven by PM H^+-ATPases (Siao et al., 2020). Vanadate (Na_3VO_4) is an inhibitor of P-type ATPase including the PM H^+-ATPase (Kinoshita and Shimazaki, 1999). We transferred 5-day-old seedlings of WT and *mns1 mns2 mns3* grown on plates at pH 6.0 to plates at pH 6.0 and pH 8.2 with different concentrations of Na_3VO_4. In the presence of increasing concentrations of Na_3VO_4, primary roots of the WT plants became progressively shorter at normal and alkaline growth conditions, and the WT plants grown under alkaline condition were more

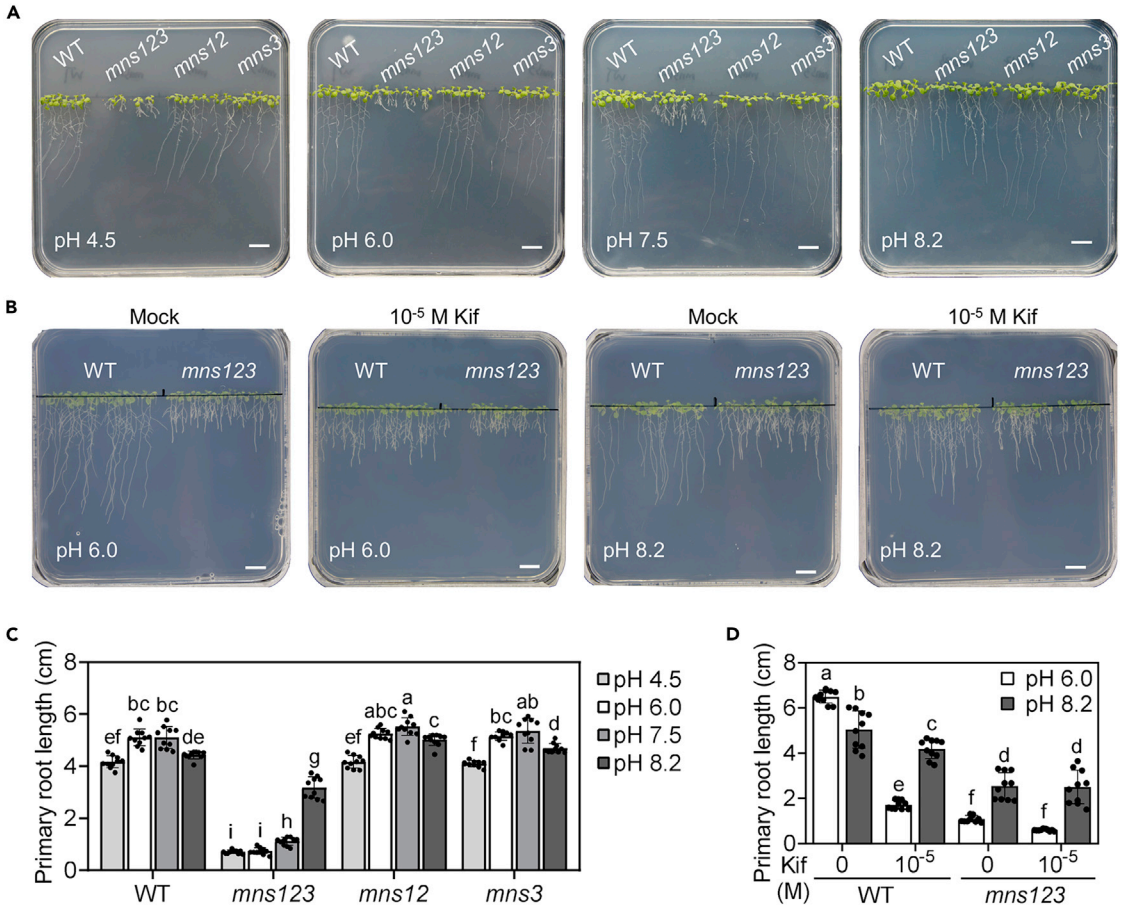

Figure 1. Short root phenotypes caused by the lack of MNS1-3 activity were partially rescued under alkaline condition (see also Figure S1)

(A) Root phenotypes of *Arabidopsis* wild type (WT, Col-0), *mns3*, *mns1 mns2* double mutant, and *mns1 mns2 mns3* triple mutant plants grown on media with different pH for 10 days *mns12* represents the *mns1 mns2* double mutant; *mns123* represents the *mns1 mns2 mns3* triple mutant; bars = 1 cm.

(B) Root phenotypes of *Arabidopsis* WT and *mns1 mns2 mns3* triple mutant plants grown on media at pH 6.0 or pH 8.2 with 0 and 10^{-5} M kifunensine (Kif) for 10 days. Bars = 1 cm.

(C and D) Statistic analyses of the primary root length in (A) and (B), respectively. Error bars represent SE (n = 10), one-way ANOVA test was used to determine statistical significance, and significant differences ($p < 0.05$) were indicated by different lowercase letters.

sensitive to Na_3VO_4 treatment than those grown under normal condition (Figures 2B and 2C). Na_3VO_4 also inhibited the root elongation of the *mns1 mns2 mns3* mutant at normal and alkaline conditions, and the alkaline-maintained root growth in *mns1 mns2 mns3* was completely suppressed when treated with 10^{-4} M Na_3VO_4 (Figures 2B and 2C). This implied that PM H^+-ATPase activity was insufficient for alkaline-maintained root growth in the *mns1 mns2 mns3* triple mutant.

Auxin transport was involved in the alkaline-maintained root growth of the *mns1 mns2 mns3* mutant

Our previous studies showed that auxin transport plays an important role in the adaptation of *Arabidopsis* roots to alkaline stress by mediating proton secretion (Xu et al., 2012). Thus, we determined the root phenotypes of the WT and *mns1 mns2 mns3* mutant grown on media at pH 6.0 and 8.2 with different concentrations of auxin transport inhibitors 1-naphthylphthalamidic acid (NPA) or 2,3,5-triiodobenzoic acid (TIBA). Application of different concentrations of NPA progressively inhibited the WT root growth under normal and alkaline conditions, and the WT plants were more sensitive to NPA treatment when grown under alkaline condition; by contrast, the root growth of the *mns1 mns2 mns3* mutant was extremely inhibited with or without NPA under pH 6.0, and suppressed progressively with the increase in NPA concentrations under pH 8.2 (Figures 3A and 3B). Similar but slightly different results were observed when TIBA was used; the

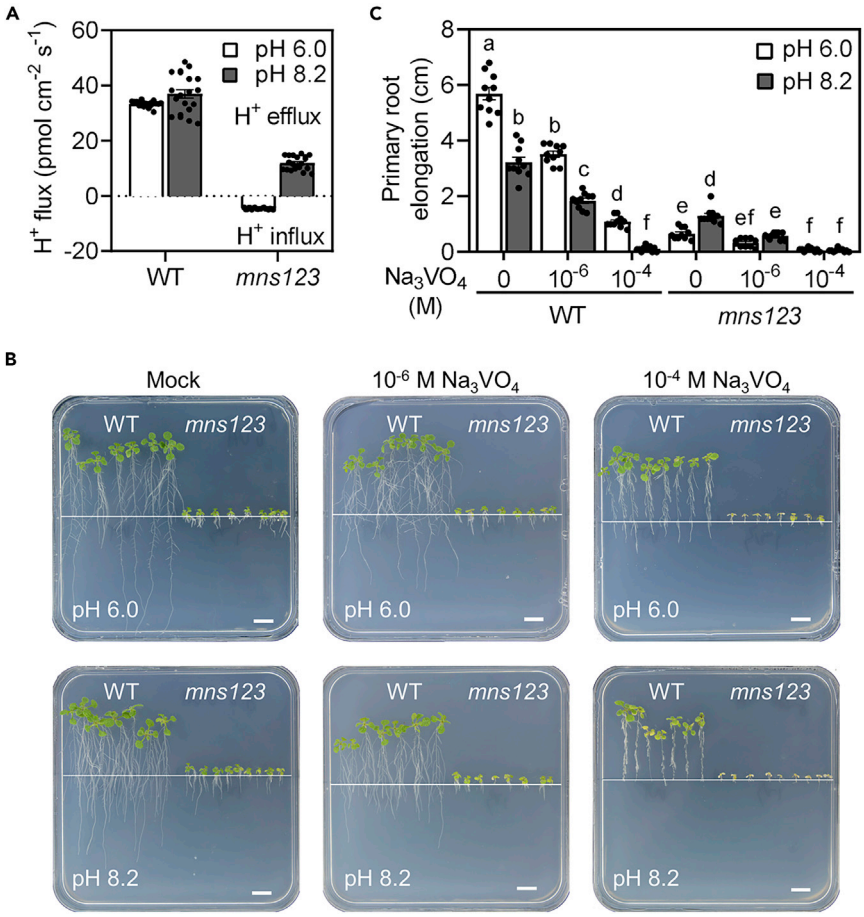

Figure 2. Proton secretion in the root tips of the *mns1 mns2 mns3* mutant recovered under alkaline condition

(A) Net proton fluxes in the primary root elongation zone of the 10-day-old WT and *mns1 mns2 mns3* triple mutant grown on media at pH 6.0 or pH 8.2. Error bars represent SE (n = 20).

(B) Five-day-old WT and *mns1 mns2 mns3* seedlings, germinated on media pH 6.0, were transferred to plates at pH 6.0 or pH 8.2 with 0, 10^{-6}, and 10^{-4} M Na_3VO_4. Root phenotypes were recorded 5 days after seedling transfer. Bars = 1 cm.

(C) Primary root elongation in (B) was measured 5 days after seedling transfer. Error bars represent SE (n = 10), one-way ANOVA test was used to determine statistical significance, and significant differences ($p < 0.05$) were indicated by different lowercase letters.

WT plants were not more sensitive to TIBA treatments when grown under pH 8.2 compared to those under pH 6.0, and the root growth of the *mns1 mns2 mns3* mutant was completely suppressed when treated with 10^{-6} M TIBA under pH 8.2 (Figure 3D). The results suggested that polar auxin transport was involved in the alkaline-maintained root growth in the *mns1 mns2 mns3* mutant.

N-glycoproteome of the *mns1 mns2 mns3* mutant was affected by alkaline stress

To further uncover the molecular mechanism of the alkaline-maintained root growth in *mns1 mns2 mns3*, we performed a quantitative N-glycoproteomic analysis by using N-glycoproteomic pipeline consisting of hydrophilic interaction chromatography (HILIC)-based N-glycopeptide enrichment, ^{18}O-labeling of *in vivo* N-glycosylation sites, and liquid chromatography-tandem mass spectrometry (LC-MS/MS). The 10-day-old seedling roots of the WT and *mns1 mns2 mns3* grown on 1/2 MS medium at pH 6.0 and pH 8.2 were used. For three biological replicates, we identified a total of 4736 N-glycosite-containing peptides (termed N-glycopeptides), corresponding to 2069 distinct N-glycopeptides from 1139 unique N-glycoproteins (Table S1; Data S1). Among them, 1486 N-glycopeptides from 910 N-glycoproteins are quantifiable in at least one biological replicate (Table S1; Data S1). Recently, Zielinska et al. (2012) identified 2186 N-glycopeptides from 1240 N-glycoproteins in *Arabidopsis* by using the N-glyco-filter-aided sample

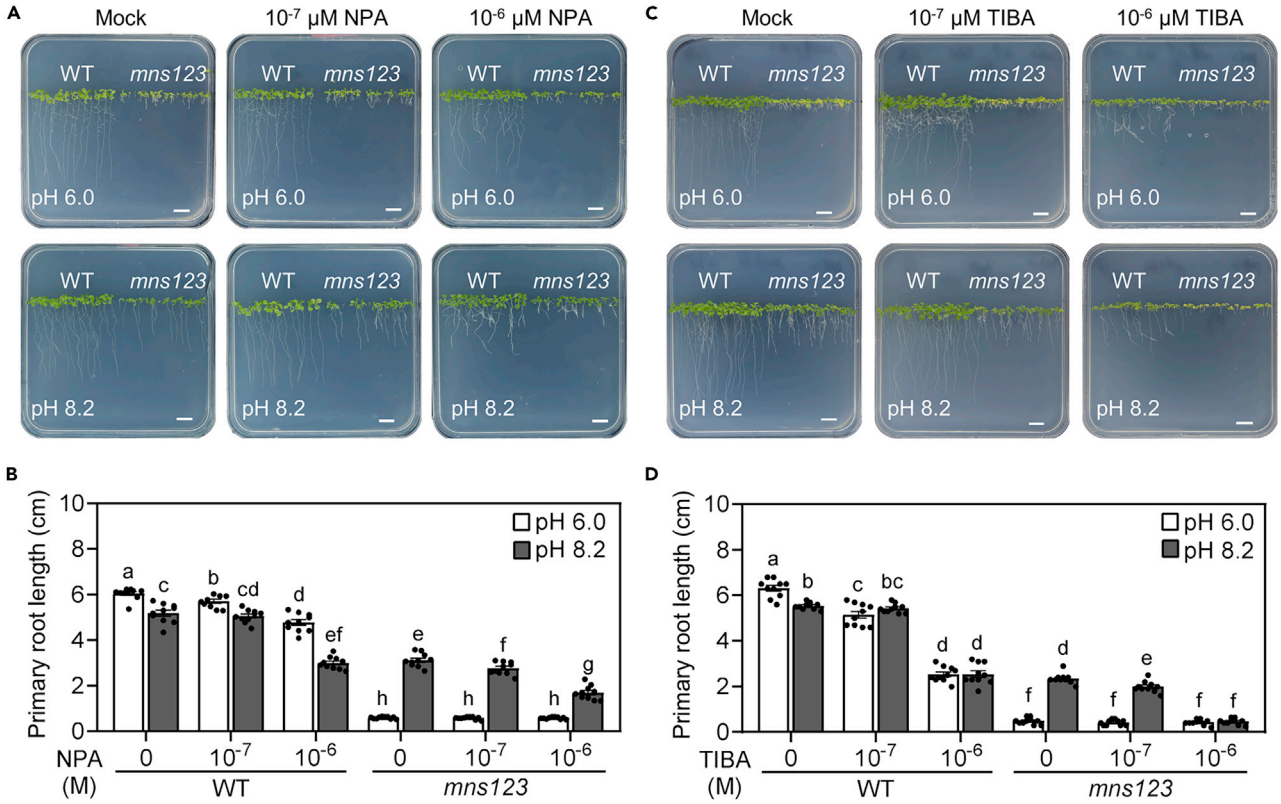

Figure 3. NPA and TIBA inhibited the alkaline-maintained root growth in the *mns1 mns2 mns3* mutant

(A) Root phenotypes of the WT and *mns1 mns2 mns3* grown on media at pH 6.0 or pH 8.2 with 0, 10^{-7}, and 10^{-6} M NPA for 10 days. NPA, 1-naphthylphthalamidic acid; bars = 1 cm.

(B) Statistic analysis of the primary root length in (A).

(C) Root phenotypes of the WT and *mns1 mns2 mns3* grown on media at pH 6.0 or pH 8.2 with 0, 10^{-7}, and 10^{-6} M TIBA for 10 days. TIBA, 2,3,5-triiodobenzoic acid; bars = 1 cm.

(D) Statistic analysis of the primary root length in (C). Error bars represent SE (n = 10 for B and C), one-way ANOVA test was used to determine statistical significance, and significant differences ($p < 0.05$) were indicated by different lowercase letters.

preparation (FASP) method (Zielinska et al., 2012). We marked the N-glycoproteins overlap between our results and those of Zielinska's, 828 N-glycopeptides from 538 N-glycoproteins in Zielinska's data were detected in our N-glycoproteomic profile (Data S1).

Given that we used PNGase F-catalyzed glycosylation site ^{18}O-labeling method for relative N-glycopeptide quantitation, an enzyme that cleaves N-glycans lacking core fucose residues, apparent increased N-glycopeptide abundance was observed due to the prevention of α-1,3-fucosylation in the *mns1 mns2 mns3* mutant. Thus, we only compared the N-glycopeptide abundance between high and normal pH with the same genotype; the significant difference was set as fold change >1.3 or <1/1.3, $p < 0.05$, unpaired two-tailed Student's *t* test (Table S2; Data S1). In the *mns1 mns2 mns3* mutant, we identified 144 N-glycopeptides from 122 N-glycoproteins with decreased abundance and 105 N-glycopeptides from 77 N-glycoproteins with increased abundance (Table S2). Gene ontology (GO) enrichment analysis of these differential N-glycoproteins showed that the enriched biological processes were response to stress (GO:0006950), cell wall organization (GO:0071555), and secondary metabolic process (GO:0019748) (Data S2). By contrast, 16 N-glycopeptides from 15 N-glycoproteins with decreased abundance and 32 N-glycopeptides from 29 N-glycoproteins with increased abundance were identified in the WT (Table S1); the enriched biological process of these differential N-glycoproteins was growth (GO:0040007) (Data S3).

Auxin homeostasis was altered by alkaline stress in the *mns1 mns2 mns3* mutant

As mentioned above, auxin transport was related to the alkaline-maintained root growth in the *mns1 mns2 mns3* mutant (Figure 3). Therefore, auxin-related N-glycoproteins in our N-glycoproteomic data were

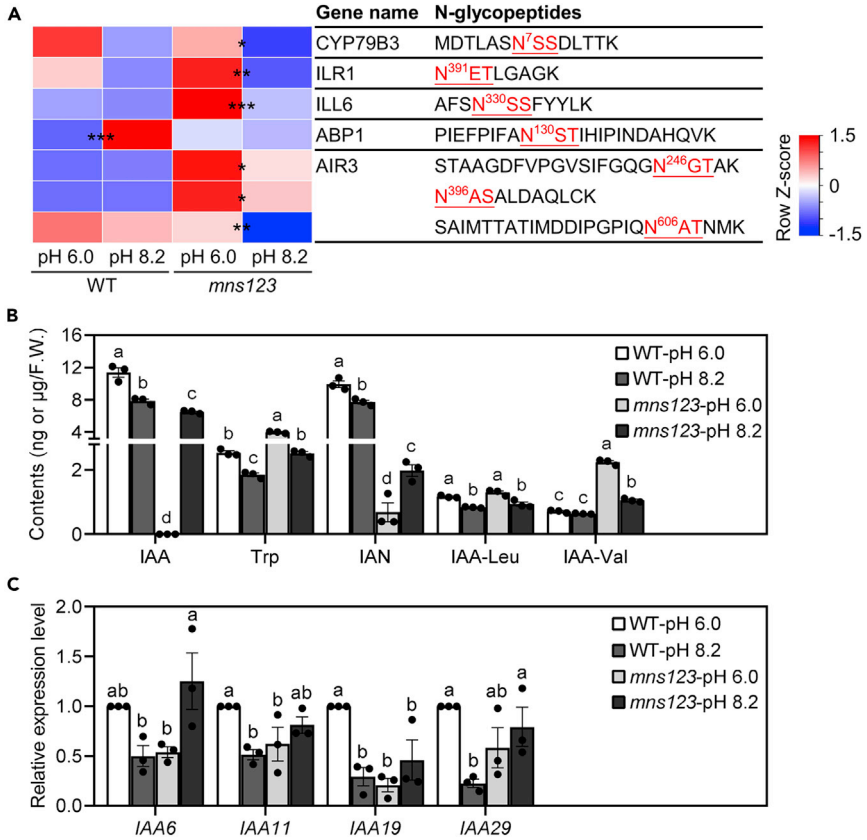

Figure 4. Auxin homeostasis was affected by alkaline treatment in the *mns1 mns2 mns3* mutant

(A) The differential abundance of auxin-related N-glycopeptides between normal (pH 6.0) and alkaline growth conditions (pH 8.2) in the WT or *mns1 mns2 mns3* mutant. The color of each cell indicates the normalized N-glycopeptide abundance scaled by row. The N-glycosylation sequon "NxS/T" (x ≠ proline) of each N-glycopeptide was underlined and marked in red. The significant differences are indicated *p < 0.05, **p < 0.01 and ***p < 0.001, unpaired two-tailed Student's *t* test. ILR1, IAA-LEUCINE RESISTANT1; ILL6, ILR1-like6; ABP1, AUXIN BINDING PROTEIN1; AIR3, AUXIN-INDUCED IN ROOT CULTURES3. The source data were shown in the Data S4.

(B) Contents of IAA, several of its precursors, and the IAA-amino acid conjugates in the roots of 10-day-old WT and *mns1 mns2 mns3* mutant seedlings grown under pH 6.0 or pH 8.2. IAA, indole-3-acetic acid; Trp, tryptophan; IAN, indole-3-acetonitrile; IAA-Leu, indole-3-acetyl leucine; IAA-Val, indole-3-acetyl valine. The units of IAA, IAA-Leu and IAA-Val were ng per g fresh weight (ng/g F.W.), and the units of Trp and IAN were μg per g fresh weight (μg/g F.W.). The source data were shown in the Data S5.

(C) Relative expression levels of auxin-responsive genes in the 10-day-old WT and *mns1 mns2 mns3* mutant grown under pH 6.0 or pH 8.2. Gene expression level in the WT grown under pH 6.0 was set as 1. Error bars represent SE (n = 3 for B and C), one-way ANOVA test was used to determine statistical significance, and significant differences ($p < 0.05$) were indicated by different lowercase letters.

analyzed. Several N-glycopeptides associated with auxin biosynthesis, amino acid conjugates hydrolysis, and response showed differential abundance between normal and alkaline conditions (Figure 4A; Data S4). For example, N-glycopeptides of CYP79B3 containing with N^{7}SS, IAA-LEUCINE RESISTANT1 (ILR1) containing with N^{391}ET, ILR1-like6 (ILL6) containing with N^{330}SS and AUXIN-INDUCED IN ROOT CULTURES3 (AIR3) containing with N^{246}GT, N^{396}AS, and N^{606}AT showed decreased abundance in the *mns1 mns2 mns3* mutant grown at pH 8.2 compared to those grown at pH 6.0 (Figure 4A). *CYP79B3* encodes a cytochrome P450 enzyme that catalyzes the conversion of tryptophan (Trp) to indole-3-acetaldoxime (IAOx), an important intermediate in auxin biosynthesis (Zhao et al., 2002); ILR1 is an amidohydrolase that releases active indole-3-acetic acid (IAA) from IAA-amino acid (IAA-aa) conjugates (Bartel and Fink, 1995; Sanchez Carranza et al., 2016); AIR3 encodes an extracellular subtilisin-like serine protease which is activated during auxin-induced lateral root formation (Neuteboom et al., 1999a). In addition, N-glycopeptide of AUXIN BINDING PROTEIN1 (ABP1) containing with N^{130}ST showed increased

abundance in the WT between normal and alkaline conditions (Figure 4A). ABP1 has the auxin binding capacity whose gain-of-function mutant generates a broad range of auxin-related phenotypes (Gelová et al., 2021).

We hypothesized that aberrant auxin abundance via synthesis or release from IAA-aa conjugates, as indicated by auxin-related N-glycopeptides, might interfere with auxin homeostasis. To test this, contents of IAA, several of its precursors, and the IAA-aa conjugates were measured in the roots of 10-day-old WT and *mns1 mns2 mns3* mutant seedlings grown under pH 6.0 and pH 8.2 (Data S5). IAA content in the *mns1 mns2 mns3* mutant was too low to be detected under pH 6.0 and 6.5 $\pm$ 0.2 ng/g fresh weight (F.W.) under pH 8.2, whereas IAA content in WT under pH 8.2 was 69% of that under pH 6.0 (Figure 4B). In addition, the changes of indole-3-acetonitrile (IAN), a direct precursor of IAA, were similar to those of IAA; the content of Trp in the *mns1 mns2 mns3* mutant under pH 6.0 showed the highest level among the four experimental groups; the contents of IAA-leucine (IAA-Leu) and IAA-valine (IAA-Val) in the *mns1 mns2 mns3* mutant plants grown at pH 8.2 were lower than those grown at pH 6.0 (Figure 4B).

To examine whether altered auxin homeostasis led to perturbed gene expression, we also analyzed the expression of auxin-responsive genes at the roots of 10-day-old WT and *mns1 mns2 mns3* seedlings grown at pH 6.0 and pH 8.2. The expression levels of *Auxin/Indole-3-Acetic Acid* (*Aux/IAA*) genes *IAA11* and *IAA19* were lower in the *mns1 mns2 mns3* mutant than in the WT under pH 6.0, whereas the expression level of *IAA6* was increased in *mns1 mns2 mns3* under pH 8.2 compared to that under pH 6.0 (Figure 4C). Overall, these results revealed that no IAA detected in the *mns1 mns2 mns3* mutant at pH 6.0 indicated lower IAA transport into the root elongation zone, resulting in altered auxin signaling and gene expression, which was revoked at pH 8.2, when auxin was detected again.

DISCUSSION

In eukaryotes, protein N-glycosylation is one of the most important co- and post-translational modifications and involves large number of enzymes that are necessary for the synthesis and maturation of glycans linked with N residues of the nascent polypeptides (Nagashima et al., 2018). MNS1-3 together is responsible for N-glycan processing from $Man_9GlcNAc_2$ to $Man_5GlcNAc_2$, which is a prerequisite for complex N-glycan formation in the Golgi apparatus (Strasser, 2014). Only the *mns1 mns2 mns3* triple mutant instead of *mns3* or the *mns1 mns2* double mutant exhibited severe root phenotypes when grown on MS media without sucrose at normal growth condition (Figure 1A) (Liebminger et al., 2009; Strasser, 2014), but the underlying processes and affected N-glycoproteins have not been discovered yet. Recent studies reported that the formation of complex N-glycans is still possible in *mns3*, but there are also additional N-glycans that are not present in WT, while the *mns1 mns2* and *mns1 mns2 mns3* mutants accumulate $Man_8GlcNAc_2$ and $Man_9GlcNAc_2$, respectively (Liebminger et al., 2009). Correctly folded N-glycoproteins with $Man_8GlcNAc_2$ can be successfully released from ER quality control (ERQC) and arrive at the *cis*-Golgi; by contrast, N-glycoproteins with the $Man_9GlcNAc_2$ structure were retained on the ER, leading to the possibility of enhanced ER-associated degradation (ERAD) (Hüttner et al., 2014; Schoberer et al., 2019). Veit et al. (2018) revealed that ectopic expression of MNS1 targeting to the *trans*-Golgi results in a considerable amount of $Man_9GlcNAc_2$ being processed to $Man_8GlcNAc_2$ and is sufficient to rescue the root growth defect in the *mns1 mns2 mns3* mutant, indicating that processing of terminal mannose residues from oligomannosidic N-glycans is crucial for an unknown late- or post-Golgi process that is essential for proper root growth (Veit et al., 2018).

In the current study, we found that the root growth inhibition of the *mns1 mns2 mns3* mutant was partially rescued when grown on medium at high pH, indicating a potential role of MNSs-mediated α-1,2-mannose trimming of N-glycan in alkaline response (Figure 1). Auxin and proton secretion are the important parts of alkaline adaptation in *Arabido*psis (Gujas et al., 2012; Xu et al., 2012, 2013). We found a conversion of proton flux from inward to outward in the *mns1 mns2 mns3* mutant under alkaline condition, and inhibitor treatment to disrupt auxin polar transport counteracted the alkaline-maintained root growth in *mns* triple mutant. Further measurement of auxin contents showed an increase in free IAA content in the *mns1 mns2 mns3* mutant at alkaline pH compared to the extremely low content of IAA under normal pH (Figure 4B), and downregulation of N-glycopeptide abundance of ILR1 and ILL6 that can release IAA from amino acid conjugates nicely matches this IAA recovery in the *mns1 mns2 mns3* mutant under alkaline condition (Figure 4A). Recent studies reported that N-glycosylation plays an important role in auxin level and transport in rice. Mutation of α-1,3-fucosyltransferase that catalyzes the transfer of fucose from GDP-fucose

to N-linked GlcNAc in medial Golgi led to reduced basipetal auxin transport and low auxin accumulation at the base of the shoot in rice (Harmoko et al., 2016). Reduced auxin level and acropetal transport were also observed in the root of the rice *osmogs* mutant which contains a point mutation in a mannosyl-oligosaccharide glucosidase, an ortholog of GCS1/KNOPF in *Arabidopsis* that catalyzes the first N-glycan trimming step and is involved in ERQC. In fact, underglycosylation of auxin efflux carriers OsABCB2 and OsABCB14 seems to be linked to reduce auxin transport in the *osmogs* mutant (Wang et al., 2014). This made us hypothesize that in the *mns1 mns2 mns3* mutant untrimmed terminal mannoses might cause auxin-related N-glycoproteins (e.g., ABCBs) retention in the ER and elimination by ERAD, thus leading to the undetectable IAA level under normal condition.

In addition, CYP79B3 appears to be glycosylated at the N7 residue (Figure 4A), indicating that the N terminus of CYP79B3 is not cleaved and luminally oriented in the ER, thus accessible to glycosyltransferases. Consistently, when a sequence of 29 amino acids that contains an N-glycosylation site at N9 residue was attached to the N terminus of rabbit cytochrome P450 2C1, the hybrid protein was able to be glycosylated *in vitro* and *in vivo* (Szczesna-Skorupa and Kemper, 1993). Gain-of-function and loss-of-function mutations in *CYP79B3* and its homolog *CYP79B2* have a corresponding increase and decrease in levels of IAA and its metabolites (Zhao et al., 2002). In our data, N-glycopeptide abundance of CYP79B3 with N7 residue was downregulated between the alkaline and normal growth conditions in the *mns* triple mutant, the same trend was also found in WT (Figure 4A). This is unable to explain the different changes in IAA levels between alkaline and normal conditions in the WT and *mns1 mns2 mns3* mutant. Further characterizing the relevance of N-glycan processing for CYP79B3 biological function and other candidate N-glycoproteins might be helpful to unravel this puzzle.

AIR3 encodes a subtilisin-like protease that might weaken cell-to-cell connections to facilitate lateral root emergence (Neuteboom et al., 1999b). In our data, abundance of three N-glycopeptides of AIR3 also showed decreased levels in the *mns1 mns2 mns3* mutant after alkaline treatment, the same but not significant trends were observed in WT (Figure 4A). To investigate whether aberrant abundance of AIR3 N-glycopeptides affects the development of lateral root, we determined the lateral root number and density of the WT and *mns1 mns2 mns3* mutant under pH 6.0 and pH 8.2. As shown in Figure S2, the lateral root number and density of the *mns1 mns2 mns3* mutant were significantly increased and decreased after alkaline treatment, whereas those of the WT were unchanged (Figure S2). This indicated that not only the primary root growth but also the lateral root development was influenced by alkaline pH in the *mns1 mns2 mns3* triple mutant.

Overall, we tried to interpret the phenomenon of alkaline-maintained root growth in the *mns1 mns2 mns3* mutant in the light of acid growth theory: under the normal growth condition (pH 6.0), too low auxin levels (albeit proton influx) led to inhibition of root growth in the *mns* triple mutant; whereas under alkaline conditions (pH 8.2), the abundance of auxin homeostasis-related N-glycopeptides was altered, auxin levels recovered concomitant with proton extrusion into the apoplast, which was able to maintain root growth of the *mns1 mns2 mns3* mutant (Figure 5).

Limitations of the study

A limitation of the study is that our quantitative N-glycoproteome analysis only identified the differential N-glycopeptide abundance between normal and alkaline growth conditions with the same genotype, but not between the WT and *mns1 mns2 mns3* mutant. Moreover, it is unclear whether the observed changes in N-glycopeptide abundance were due to altered protein expression or altered N-glycosylation site occupancy. Further investigations of the N-glycosylation status and expression of candidate N-glycoproteins (e.g., Western blotting) in the WT and *mns* triple mutant at pH 6.0 and pH 8.2 might be helpful to elucidate this confusion. Therefore, the study presented here should be considered as a starting point for the unraveling of the underlying molecular mechanisms of N-glycan processing in the response of alkaline stress in *Arabidopsis*.

STAR★METHODS

Detailed methods are provided in the online version of this paper and include the following:

- KEY RESOURCES TABLE
- RESOURCE AVAILABILITY

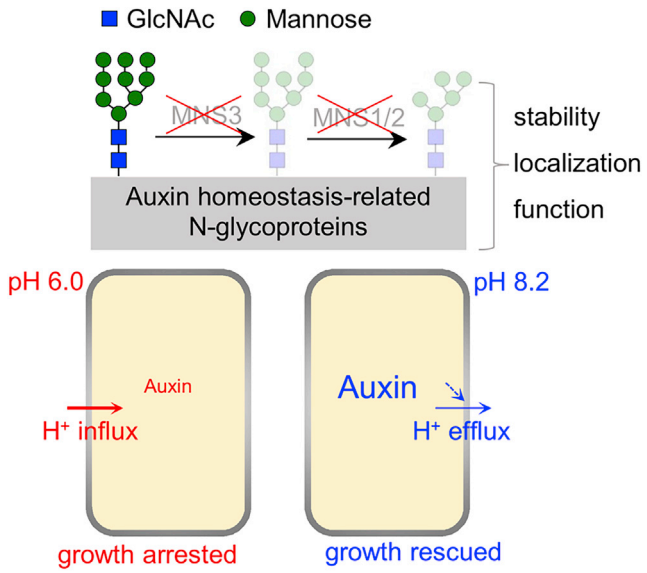

Figure 5. Proposed model of the alkaline-maintained root growth in the *mns1 mns2 mns3* mutant

Mutations of MNS1-3 led to the N-glycan structures of most N-glycoproteins as $Man_9GlcNAc_2$, including auxin homeostasis-related N-glycoproteins, which probably affect their stability, localization, and/or function. Under pH 6.0 (marked in red), the auxin level in the root cells of the *mns1 mns2 mns3* mutant was extremely low and a proton influx was observed, leading to inhibition of root growth. Under pH 8.2 (marked in blue), the auxin level was recovered probably due to the attenuated abundance of auxin homeostasis-related N-glycopeptides, which induces proton extrusion and rescues the root growth partially. GlcNAc represents N-acetylglucosamine.

- Lead contact
- Materials availability
- Data and code availability
- EXPERIMENTAL MODEL AND SUBJECT DETAILS
  - Plant materials and growth conditions
- METHOD DETAILS
  - Pharmacological treatments
  - Phenotypic analyses
  - Measurement of net H^+ flux with the SIET system
  - Protein extraction, digestion and TMT peptide labeling
  - Glycopeptide enrichment and ^{18}O labeling of N-glycosites
  - LC-MS/MS based N-glycoproteomic analysis
  - Quantification and differential analysis of N-glycopeptide abundance
  - Quantification of IAA and its metabolites
  - RNA extraction and qRT-PCR
- QUANTIFICATION AND STATISTICAL ANALYSIS

SUPPLEMENTAL INFORMATION

Supplemental information can be found online at https://doi.org/10.1016/j.isci.2022.104298.

ACKNOWLEDGMENTS

We are grateful for grant support from the National Key R&D Program of China (2017YFE0118100), the National Natural Science Foundation of China (31872169, 31761130073 and 31422047), a Newton Advanced Fellowship (NSFC-RS: NA160430).

AUTHOR CONTRIBUTIONS

W.X. and T.X. designed the experiments and wrote the paper; T.X., Y.Z., and Y.M. conducted the experiments and analyzed the data. J.Z. participated in data interpretation.

DECLARATION OF INTERESTS

The authors declare no competing interests.

Received: August 23, 2021
Revised: November 30, 2021
Accepted: April 21, 2022
Published: May 20, 2022

REFERENCES

Bartel, B., and Fink, G.R. (1995). ILR1, an amidohydrolase that releases active indole-3-acetic acid from conjugates. Science *268*, 1745–1748. https://doi.org/10.1126/science.7792599.

Fuglsang, A.T., Guo, Y., Cuin, T.A., Qiu, Q., Song, C., Kristiansen, K.A., Bych, K., Schulz, A., Shabala, S., Schumaker, K.S., et al. (2007). *Arabidopsis* protein kinase PKS5 inhibits the plasma membrane H^+-ATPase by preventing interaction with 14-3-3 protein. Plant Cell *19*, 1617–1634. https://doi.org/10.1105/tpc.105.035626.

Gelová, Z., Gallei, M., Pernisová, M., Brunoud, G., Zhang, X., Glanc, M., Li, L., Michalko, J., Pavlovičová, Z., Verstraeten, I., et al. (2021). Developmental roles of auxin binding protein 1 in *Arabidopsis thaliana*. Plant Sci. *303*, 110750. https://doi.org/10.1016/j.plantsci.2020.110750.

Gujas, B., Alonso-Blanco, C., and Hardtke, Christian S. (2012). Natural *Arabidopsis brx* loss-of-function alleles confer root adaptation to acidic soil. Curr. Biol. *22*, 1962–1968. https://doi.org/10.1016/j.cub.2012.08.026.

Guo, R., Shi, L., Ding, X., Hu, Y., Tian, S., Yan, D., Shao, S., Gao, Y., Liu, R., and Yang, Y. (2010). Effects of saline and alkaline stress on germination, seedling growth, and ion balance in wheat. Agron. J. *102*, 1252–1260. https://doi.org/10.2134/agronj2010.0022.

Harmoko, R., Yoo, J.Y., Ko, K.S., Ramasamy, N.K., Hwang, B.Y., Lee, E.J., Kim, Ho S., Lee, K.J., Oh, D.-B., Kim, D.Y., et al. (2016). N-glycan containing a core α1,3-fucose residue is required for basipetal auxin transport and gravitropic response in rice (*Oryza sativa*). New Phytol. *212*, 108–122. https://doi.org/10.1111/nph.14031.

Helenius, A., and Aebi, M. (2001). Intracellular functions of N-linked glycans. Science *291*, 2364–2369. https://doi.org/10.1126/science.291.5512.2364.

Hüttner, S., Veit, C., Vavra, U., Schoberer, J., Liebminger, E., Maresch, D., Grass, J., Altmann, F., Mach, L., and Strasser, R. (2014). *Arabidopsis* class I α-mannosidases MNS4 and MNS5 are involved in endoplasmic reticulum-associated degradation of misfolded glycoproteins. Plant Cell *26*, 1712–1728. https://doi.org/10.1105/tpc.114.123216.

Kinoshita, T., and Shimazaki, K. (1999). Blue light activates the plasma membrane H^+-ATPase by phosphorylation of the C-terminus in stomatal guard cells. EMBO J. *18*, 5548–5558. https://doi.org/10.1093/emboj/18.20.5548.

Kornfeld, R., and Kornfeld, S. (1985). Assembly of asparagine-linked oligosaccharides. Annu. Rev. Biochem. *54*, 631–664. https://doi.org/10.1146/annurev.bi.54.070185.003215.

Ladwig, F., Dahlke, R.I., Stührwohldt, N., Hartmann, J., Harter, K., and Sauter, M. (2015). Phytosulfokine regulates growth in *Arabidopsis* through a response module at the plasma membrane that includes CYCLIC NUCLEOTIDE-GATED CHANNEL17, H^+-ATPase, and BAK1. Plant Cell *27*, 1718–1729. https://doi.org/10.1105/tpc.15.00306.

Liebminger, E., Hüttner, S., Vavra, U., Fischl, R., Schoberer, J., Grass, J., Blaukopf, C., Seifert, G.J., Altmann, F., Mach, L., and Strasser, R. (2009). Class I α-mannosidases are required for N-glycan processing and root development in *Arabidopsis thaliana*. Plant Cell *21*, 3850–3867. https://doi.org/10.1105/tpc.109.072363.

Liu, C., Niu, G., Zhang, H., Sun, Y., Sun, S., Yu, F., Lu, S., Yang, Y., Li, J., and Hong, Z. (2018). Trimming of N-glycans by the Golgi-localized α-1,2-mannosidases, MNS1 and MNS2, is crucial for maintaining RSW2 protein abundance during salt stress in *Arabidopsis*. Mol. Plant *11*, 678–690. https://doi.org/10.1016/j.molp.2018.01.006.

Nagashima, Y., von Schaewen, A., and Koiwa, H. (2018). Function of N-glycosylation in plants. Plant Sci. *274*, 70–79. https://doi.org/10.1016/j.plantsci.2018.05.007.

Neuteboom, L.W., Ng, J.M.Y., Kuyper, M., Clijdesdale, O.R., Hooykaas, P.J.J., and van der Zaal, B.J. (1999a). Isolation and characterization of cDNA clones corresponding with mRNAs that accumulate during auxin-induced lateral root formation. Plant Mol. Biol. *39*, 273–287. https://doi.org/10.1023/a:1006104205959.

Neuteboom, L.W., Veth-Tello, L.M., Clijdesdale, O.R., Hooykaas, P.J., and van der Zaal, B.J. (1999b). A novel subtilisin-like protease gene from *Arabidopsis thaliana* is expressed at sites of lateral root emergence. DNA Res. *6*, 13–19. https://doi.org/10.1093/dnares/6.1.13.

Sanchez Carranza, A.P., Singh, A., Steinberger, K., Panigrahi, K., Palme, K., Dovzhenko, A., and Dal Bosco, C. (2016). Hydrolases of the ILR1-like family of *Arabidopsis thaliana* modulate auxin response by regulating auxin homeostasis in the endoplasmic reticulum. Sci. Rep. *6*, 24212. https://doi.org/10.1038/srep24212.

Schoberer, J., König, J., Veit, C., Vavra, U., Liebminger, E., Botchway, S.W., Altmann, F., Kriechbaumer, V., Hawes, C., and Strasser, R. (2019). A signal motif retains *Arabidopsis* ER-α-mannosidase I in the *cis*-Golgi and prevents enhanced glycoprotein ERAD. Nat. Commun. *10*, 3701. https://doi.org/10.1038/s41467-019-11686-9.

Siao, W., Coskun, D., Baluška, F., Kronzucker, H.J., and Xu, W. (2020). Root-apex proton fluxes at the centre of soil-stress acclimation. Trends Plant Sci. *25*, 794–804. https://doi.org/10.1016/j.tplants.2020.03.002.

Spartz, A.K., Ren, H., Park, M.Y., Grandt, K.N., Lee, S.H., Murphy, A.S., Sussman, M.R., Overvoorde, P.J., and Gray, W.M. (2014). SAUR inhibition of PP2C-D phosphatases activates plasma membrane H^+-ATPases to promote cell expansion in *Arabidopsis*. Plant Cell *26*, 2129–2142. https://doi.org/10.1105/tpc.114.126037.

Strasser, R. (2014). Biological significance of complex N-glycans in plants and their impact on plant physiology. Front. Plant Sci. *5*, 363. https://doi.org/10.3389/fpls.2014.00363.

Szczesna-Skorupa, E., and Kemper, B. (1993). An N-terminal glycosylation signal on cytochrome P450 is restricted to the endoplasmic reticulum in a luminal orientation. J. Biol. Chem. *268*, 1757–1762. https://doi.org/10.1016/s0021-9258(18)53917-x.

Takahashi, K., Hayashi, K.I., and Kinoshita, T. (2012). Auxin activates the plasma membrane H^+-ATPase by phosphorylation during hypocotyl elongation in *Arabidopsis*. Plant Physiol. *159*, 632–641. https://doi.org/10.1104/pp.112.196428.

Tokunaga, F., Brostrom, C., Koide, T., and Arvan, P. (2000). Endoplasmic reticulum (ER)-associated degradation of misfolded N-linked glycoproteins is suppressed upon inhibition of ER mannosidase I. J. Biol. Chem. *275*, 40757–40764. https://doi.org/10.1074/jbc.m001073200.

Veit, C., König, J., Altmann, F., and Strasser, R. (2018). Processing of the terminal alpha-1,2-linked mannose residues from oligomannosidic N-glycans is critical for proper root growth. Front. Plant Sci. *9*, 1807. https://doi.org/10.3389/fpls.2018.01807.

Wang, S., Xu, Y., Li, Z., Zhang, S., Lim, J.M., Lee, K.O., Li, C., Qian, Q., Jiang, D.A., and Qi, Y. (2014). OsMOGS is required for *N*-glycan formation and auxin-mediated root development in rice (*Oryza sativa* L.). Plant J. *78*, 632–645. https://doi.org/10.1111/tpj.12497.

Xu, W., Jia, L., Baluška, F., Ding, G., Shi, W., Ye, N., and Zhang, J. (2012). PIN2 is required for the adaptation of *Arabidopsis* roots to alkaline stress by modulating proton secretion. J. Exp. Bot. *63*, 6105–6114. https://doi.org/10.1093/jxb/ers259.

Xu, W., Jia, L., Shi, W., Baluˌka, F., Kronzucker, H.J., Liang, J., and Zhang, J. (2013). The tomato 14-3-3 protein TFT4 modulates H+ efflux, basipetal auxin transport, and the PKS5-J3 pathway in the root growth response to alkaline stress. Plant Physiol. *163*, 1817–1828. https://doi.org/10.1104/pp.113.224758.

Yang, Y., Qin, Y., Xie, C., Zhao, F., Zhao, J., Liu, D., Chen, S., Fuglsang, A.T., Palmgren, M.G., Schumaker, K.S., et al. (2010). The *Arabidopsis* chaperone J3 regulates the plasma membrane H^+-ATPase through interaction with the PKS5 kinase. Plant Cell *22*, 1313–1332. https://doi.org/10.1105/tpc.109.069609.

Zhao, Y., Hull, A.K., Gupta, N.R., Goss, K.A., Alonso, J., Ecker, J.R., Normanly, J., Chory, J., and Celenza, J.L. (2002). Trp-dependent auxin biosynthesis in *Arabidopsis*: involvement of cytochrome P450s CYP79B2 and CYP79B3. Genes Dev. *16*, 3100–3112. https://doi.org/10.1101/gad.1035402.

Zielinska, Dorota F., Gnad, F., Schropp, K., Wiśniewski, Jacek R., and Mann, M. (2012). Mapping N-glycosylation sites across seven evolutionarily distant species reveals a divergent substrate proteome despite a common core machinery. Mol. Cell *46*, 542–548. https://doi.org/10.1016/j.molcel.2012.04.031.

STAR★METHODS

KEY RESOURCES TABLE

REAGENT or RESOURCE	SOURCE	IDENTIFIER
Chemicals, peptides, and recombinant proteins		
Kifunensine (Kif)	Sigma-Aldrich	CAT#K1140
Vanadate	BBI	CAT#A600869
2,3,5-triiodobenzoic acid (TIBA)	BBI	CAT#A600735
1-naphthylphthalamidic acid (NPA)	Sigma-Aldrich	CAT#33371
Trypsin from bovine pancreas	Sigma-Aldrich	CAT#T1426
Trifluoroacetic acid	Sigma-Aldrich	CAT#302031
Acetonitrile	Sigma-Aldrich	CAT#34851
$H_2{}^{18}O$	Sigma-Aldrich	CAT#329878
PNGase F	NEB	CAT#P0704
TRIzol	Thermo Fisher	CAT#15596026
Critical commercial assays		
Easy II Protein Quantitative Kit (BCA)	TransGen Biotech	CAT#DQ111-01
TransScript One-Step gDNA Removal and cDNA Synthesis SuperMix Kit	TransGen Biotech	CAT#AT311-02
AceQ qPCR SYBR Green Master Mix	Vazyme	CAT#Q111-02
Deposited data		
Arabidopsis N-glycoproteome profile	Zielinska et al. (2012)	https://doi.org/10.1016/j.molcel.2012.04.031
Experimental models: Organisms/strains		
Arabidopsis thaliana Columbia ecotype Col-0	ABRC	CS22625
Arabidopsis *mns1*	NASC	SALK_149737
Arabidopsis *mns2*	NASC	SALK_023251
Arabidopsis *mns3*	NASC	SALK_087161
Arabidopsis *mns1 mns2*	This study	Cross between *mns1* and *mns2*
Arabidopsis *mns1 mns2 mns3*	This study	Cross between *mns1 mns2* and *mns3*
Oligonucleotides		
Primers used are shown in Table S3	This study	N/A
Software and algorithms		
IBM SPSS Statistics	Statistical Analysis System	https://www.ibm.com/analytics/spss-statisticssoftware
ImageJ	NIH, USA	https://imagej.nih.gov/ij/
MaxQuant	Max-Planck Institute of Biochemistry	https://www.maxquant.org/
Proteome Discoverer	Thermo Fisher	https://www.thermofisher.com

RESOURCE AVAILABILITY

Lead contact

Further information and requests for resources and reagents should be directed to and will be fulfilled by the lead contact, Weifeng Xu (wfxu@fafu.edu.cn).

Materials availability

All materials generated in this study are available from the lead contact without restriction. This study did not generate new unique reagents.

Data and code availability

- All data supporting the conclusions are present in the paper and the supplemental information. The source data (for Figures 4A and 4B) are provided in Data S4 and S5. This paper analyzes existing, publicly available N-glycoproteome of *Arabidopsis* (Zielinska et al., 2012), and DOI is listed in the key resources table.
- This paper does not report original code.
- Any additional information required to reanalyze the data reported in this paper is available from the lead contact upon request.

EXPERIMENTAL MODEL AND SUBJECT DETAILS

Plant materials and growth conditions

Plants of the Columbia-0 (Col-0) WT genetic background and mutants were used in this study. T-DNA insertion lines *mns1* (SALK_149737), *mns2* (SALK_023251) and *mns3* (SALK_087161) were obtained from the European Arabidopsis Stock Centre. The *mns1 mns2* double mutant and *mns1 mns2 mns3* triple mutant were obtained by crossing and genotyped by PCR. Primers were listed in Table S2.

Arabidopsis seeds were surface-sterilized using 50% bleach (v/v), rinsed with sterile water five times, and sown on 1/2 Murashige and Skoog media (Caisson Labs) containing 0.8% (w/v) agar, with the pH adjusted to 6.0 via 1 M KOH or 3% HCl before adding agar and autoclaving. Note that agar is basic and slightly changes the final pH of the media, but throughout the text, pH values correspond to pH adjusted before adding agar and autoclaving. The agar plates were stratified at 4°C for 2 days before being transferred to a growth chamber maintained at 22°C under a 16-h-light/8-h-dark photoperiod.

METHOD DETAILS

Pharmacological treatments

For acidic and alkalic stress treatment, sterilized and cold-treated Col-0 and mutant seeds were germinated and grown on 1/2 MS media containing 0.8% (w/v) agar, with the pH adjusted to 4.5, 6.0, 7.5 and 8.2 before adding agar and autoclaving. For Kif, TIBA and NAA treatments, sterilized and cold-treated Col-0 and mutant seeds were germinated and grown on 1/2 MS media with or without 10^{-5} M Kif (Sigma-Aldrich), 10^{-7} M and 10^{-6} M TIBA (BBI) or NPA (Sigma-Aldrich) at pH 6.0 and pH 8.2. All plates were transferred to the growth chamber for 10 days. Primary root length was measured.

For vanadate treatments, sterilized and cold-treated Col-0 and mutant seeds were germinated and grown on 1/2 MS media at pH 6.0. The 5-day-old seedlings were then transferred to media with or without 10^{-6} M and 10^{-4} M vanadate (BBI) at pH 6.0 and pH 8.2. Primary root elongation was measured 5 days later. At least 10 seedings were used for each treatment in three independent biological replicates.

Phenotypic analyses

For root length measurements, seedlings were grown on vertically oriented medium and photographed with a Nikon D7100 camera. Total primary root length or primary root elongation were measured using ImageJ software (v.1.52). For root tip observation, the root tips were observed under bright-field illumination and photographed using a Nikon microscope P2-DBL coupled with a digital camera.

Measurement of net H^+ flux with the SIET system

Root H^+ fluxes were measured using the scanning ion-selective electrode technique (SIET) with a Noninvasive Microtest Technology System (NMT, Xuyue Sci. & Tech. Co., Ltd., Beijing, China) as described previously (Xu et al., 2012). Briefly, the roots of *Arabidopsis* plants were equilibrated in measuring solution for 20 min and then transferred to a small plastic dish (3 cm in diameter) containing 2 ml of fresh measuring solution. When the root became immobilized at the bottom of the dish, the microelectrode was vibrated in the measuring solution between 5 μm and 35 μm from the root surface, along an axis perpendicular to the root. The background was recorded by vibrating the electrode in the measuring solution not containing roots. *Arabidopsis* H^+ fluxes were measured along the root tip, concentrating on the elongation zone (520 ~ 850 μm from the root cap junction). Each plant was measured twice. The final flux values at

elongation zone were the mean of ten individual plants from each treatment. Three biological replicates were conducted.

Protein extraction, digestion and TMT peptide labeling

The 10-day-old Col-0 and *mns1 mns2 mns3* triple mutant seedling roots grown on media at pH 6.0 and pH 8.2 were used for quantitative N-glycoproteomic analysis, termed as WT grown at normal pH and high pH (npHwt and hpHwt) and *mns* triple mutant grown at normal pH and high pH (npHmns and hpHmns), respectively. Three biological replicates were conducted. Protein extraction, glycopeptide enrichment, LC-MS/MS analysis and N-glycoprotein identification and quantification were performed by PTM Biolabs (Hangzhou, China).

For protein extraction, *Arabidopsis* roots were ground by liquid nitrogen, and then four volumes of lysis buffer (8 M urea, 1% Triton-100, 10 mM dithiothreitol, and 1% Protease Inhibitor Cocktail) was added, followed by sonication three times on ice. The remaining debris was removed by centrifugation. Finally, the protein was precipitated with cold 20% TCA for 2 h at -20°C. After centrifugation, the supernatant was discarded. The remaining precipitate was washed with cold acetone and redissolved in 8 M urea. Total protein concentration was determined with BCA kit (TransGen Biotech) according to the manufacturer's instructions.

For digestion and Tandem Mass Tag (TMT) peptide labeling, protein samples were reduced with 5 mM dithiothreitol and alkylated with 11 mM iodoacetamide, and then trypsin (Sigma-Aldrich) was added at 1:50 trypsin-to-protein mass ratio for the first digestion overnight and 1:100 trypsin-to-protein mass ratio for a second 4 h-digestion. After trypsin digestion, peptide was desalted by Strata X C18 SPE column and vacuum-dried. Peptides from corresponding samples were reconstituted in 0.5 M TEAB and labeled with TMT kits according to manufacturer's protocol.

Glycopeptide enrichment and ^{18}O labeling of N-glycosites

The pooled labeled peptides were dried by vacuum centrifugation and redissolved in 5% trifluoroacetic acid (TFA, Sigma-Aldrich)/80% acetonitrile (ACN, Sigma-Aldrich). Then the peptides solution was pipetted into hydrophilic interaction chromatography (HILIC) tip that was prepacked by PTM Biolabs (Hangzhou, China). After centrifugation, the HILIC was washed with loading buffer three times. Finally, the enriched glycopeptides were eluted with H_2O and lyophilized to dryness. Purified glycopeptides were dissolved in NH_4HCO_3 prepared with $H_2{}^{18}O$ (Sigma-Aldrich) and treated with PNGase F (NEB) at 37°C overnight to allow ^{18}O-labeling of the asparagine residues at N-glycosylation sites. The ^{18}O-labeled peptides were desalted using a C18ZipTip microcolumn and dried under vacuum.

LC-MS/MS based N-glycoproteomic analysis

^{18}O-labeled N-glycosite-containing peptides from each sample were dissolved in solvent A (0.1% formic acid in 2% acetonitrile) and separated by a home-made reversed-phase column (15 cm length, 75 μm i.d.) using 40-min gradient from 6% to 80% solvent B (0.1% formic acid in 98% acetonitrile) at a flow rate of 400 nL/min on an EASY-nLC 1000 UPLC system. Data-dependent MS/MS acquisition was performed following a full MS survey scan by Orbitrap mass analyzer (m/z scan range 350 to 1800; resolution 70,000). The 20 most intense ions were fragmented by collision-induced dissociation with maximum ion accumulation time of 50 ms in the LTQ mass spectrometer (automatic gain control 50,000; dynamic exclusion 15s).

MS/MS raw data were processed using Maxquant search engine (v.1.5.2.8) to search against the *Arabidopsis thaliana* UniProt database. The following parameters were used: 20 ppm precursor ion mass tolerance; 0.02 Da fragment ion mass tolerance; trypsin digestion with up to two missed cleavages; variable modifications: asparagine deamidation in $H_2{}^{18}O$, asparagine and glutamine deamidation, methionine oxidation, and N-terminal acetylation; fixed modification: cysteine carbamidomethylation; false discovery rate (FDR) <1%.

Quantification and differential analysis of N-glycopeptide abundance

Proteome Discoverer 1.4 was used to quantify the peak area (i.e., area under the curve) of ^{18}O-labeled N-glycosite-containing peptides. The peak area of each N-glycopeptide was normalized using the formula

x_{ij}/mean(x_j), where x_{ij} indicates the peak area of each N-glycopeptide in each sample, and mean(x_j) indicates the average of all quantifiable N-glycopeptide peak area of the four samples. The normalized peak area of N-glycopeptide is used to indicate the normalized N-glycopeptide abundance. Differential abundance analyses were performed using the normalized abundance of N-glycopeptides with valid abundance values in at least two biological replicates. Significant differences were determined by using unpaired two-tailed Student's *t* test with the thresholds of >1.3 or < 1/1.3 fold change and $P < 0.05$. GO enrichment analysis was performed using the AgriGO website tool, and the significant threshold was set as $P < 0.01$ and FDR < 0.05.

Quantification of IAA and its metabolites

Roots of the WT and *mns1 mns2 mns3* mutant plants grown at pH 6.0 and pH 8.2 were harvested and homogenized in a precooled methanol/water/formic acid (15:4:1, v/v/v). The combined extracts were dried with a flow of nitrogen, redissolved in 80% methanol (v/v), and filtered through 0.22 μm filter for further LC-MS/MS analysis. The sample extracts were analyzed using an UPLC-ESI-MS/MS system (UPLC, ExionLC^{TM} AD; MS, Applied Biosystems 6500 Triple Quadrupole). Concentrations of IAA and its metabolites were quantified by MetWare (www.metware.cn/) based on the AB Sciex QTRAP 6500 LC-MS/MS platform. Three independent biological replicates were performed. The significance was determined using the unpaired two-tailed Student's *t* test with $P < 0.05$ and $|\log_2$fold change$| > 0$.

RNA extraction and qRT-PCR

Total RNA was extracted from the 10-day-old WT and *mns1 mns2 mns3* mutant roots under pH 6.0 and pH 8.2 using TRIzol reagent (Thermo Fisher Scientific) in accordance with the manufacturer's instructions. The TransScript One-Step gDNA Removal and cDNA Synthesis SuperMix Kit (TransGen Biotech) was used for cDNA synthesis, and AceQ qPCR SYBR Green Master Mix (Vazyme) was used for amplification with the Bio-Rad CFX96 real-time PCR detection system using gene-specific primer pairs (listed in Table S2). The relative expression level of genes was calculated using the $2^{\Delta\Delta Ct}$ method. *TUB6* gene was used as internal control. Experiments were performed in triplicate for each sample.

QUANTIFICATION AND STATISTICAL ANALYSIS

All the details of the statistics presented in this study are provided in the Method details section. All the data were analyzed with the analysis of variation according to SPSS software (v.24.0), and significant differences were determined by one-way ANOVA test or unpaired two-tailed Student's *t*-test at $P < 0.05$ level.